

Supporting Information

© Wiley-VCH 2013

69451 Weinheim, Germany

Supramolecular Self-Assembled Nanoparticles Mediate Oral Delivery of Therapeutic TNF- α siRNA against Systemic Inflammation**

*Lichen Yin, Ziyuan Song, Qiu hao Qu, Kyung Hoon Kim, Nan Zheng, Catherine Yao, Isthier Chaudhury, Haoyu Tang, Nathan P. Gabrielson, Fatih M. Uckun, and Jianjun Cheng**

anie_201209991_sm_miscellaneous_information.pdf

Materials, Cell Culture, and Animal Housing

TNF- α siRNA duplex and negative control siRNA containing scrambled sequences were supplied by Integrated DNA Technologies (Coralville, Iowa, USA) and dissolved in DEPC-treated water before use. The siRNA sequences were shown in Table S1. Cy3-labeled TNF- α siRNA duplex (Cy3-siRNA) was used for *in vitro* cell uptake studies, while DY800-labeled TNF- α siRNA duplex (DY800-siRNA) was used for the *in vivo* biodistribution study. Chitosan (MW = 200 kDa, deacetylation degree of 95%) was purchased from Golden-Shell Biochemical Co., Ltd. (Zhejiang, China). Boc-NH-PEG-succinimidyl valerate (Boc-PEG-SVA, MW = 3.4 kDa) was purchased from Laysan Bio (Arab, AL, USA). Dithiothreitol (DTT) was purchased from Roche Diagnostics (Indianapolis, IN, USA). *N*-hydroxysuccinimide (NHS), oleyl chloride, *N,N*-diisopropylethylamine (DIEA), cystamine dihydrochloride, D-mannosamine hydrochloride, 1,1,3,3-tetramethylguanidine, trifluoroacetic acid, lipopolysaccharide (LPS, from *E.coli* 0111:B4), and D-galactosamine (D-GalN) were purchased from Sigma-Aldrich (St. Louis, MO, USA) and used as received. Spectra/Por RC dialysis tubing with a molecular weight cut-off (MWCO) of 1 kDa was purchased from Spectrum Laboratories (Rancho Dominguez, CA, USA). PVBLG-8 was synthesized following previously published procedures.^[1]

Caco-2 cells (human colon carcinoma), Raji B cells (human Burkitt's lymphoma), and RAW 264.7 cells (mouse monocyte macrophage) were purchased from the American Type Culture Collection (Rockville, MD, USA), and cultured in DMEM supplemented with 10% fetal bovine serum (FBS).

Male C57BL/6 mice (8-10 week old) were obtained from Charles River Laboratory (Wilmington, MA, USA) and were housed in a clean room with four mice per cage. Mice were given access to water ad libitum and exposed to a 12:12 h light–dark cycle (7:00 am–7:00 pm) at 25 ± 1 °C. The animal experimental protocols were approved by the Institutional Animal Care and Use Committees of University of Illinois at Urbana–Champaign.

Supplementary Table S1. Sequence of TNF- α siRNA and Scramble siRNA

	Sequences
TNF- α sense	5'-GUCUCAGCCUCUUCUCAUUCCUGct-3'
TNF- α antisense	5'-AGCAGGAAmUGmAGmAAmGAmGGmCUmGAmGAmCmAmU-3'
Scr sense	5'-UUCUCCGAACGUGUCACGUTT-3'
Scr antisense	5'-ACGUGACACGUUCGGAGAATT-3'

Instrumentation

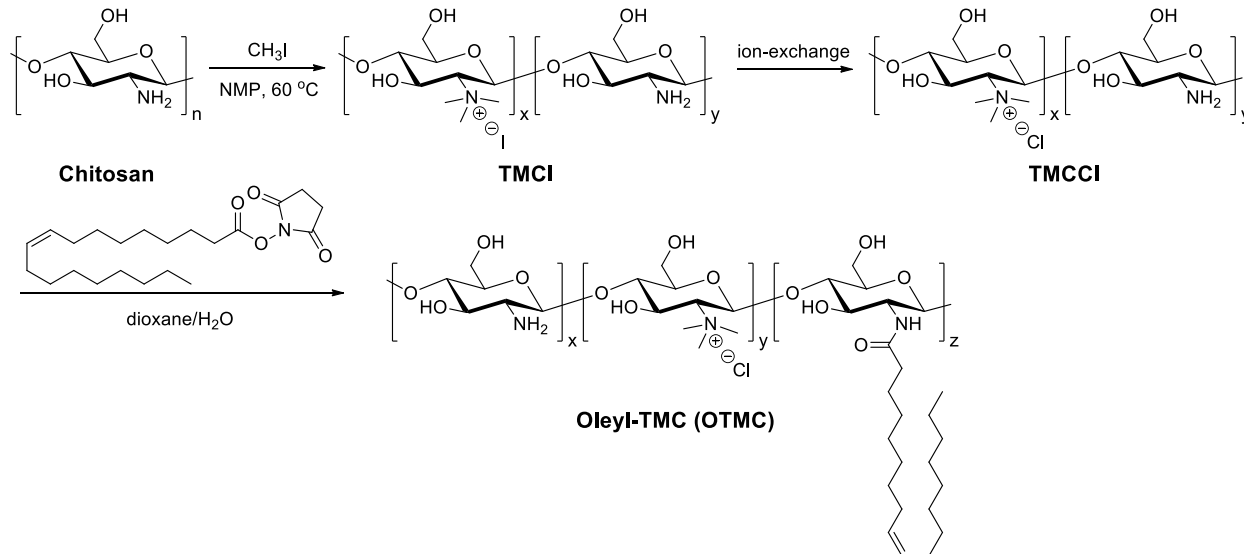
^1H NMR spectra were recorded on a Varian U500 (500 MHz) spectrometer. Electrospray Ionization mass spectrometry (ESI-MS) was performed on a Waters Quattro II Mass Spectrometer. Matrix Assisted Laser Desorption Ionization-Time Of Flight mass spectrometry (MALDI-TOF-MS) was performed on an Applied Biosystems Voyager-DE STR Time of Flight instrument or a Bruker Daltonics UltrafleXtreme MALDI-TOF instrument in positive-ion mode with 2,5-dihydroxybenzoic acid as a matrix. Gel permeation chromatography (GPC) experiments were performed on a system equipped with an isocratic pump (Model 1100, Agilent Technology, Santa Clara, CA, USA), a DAWN HELEOS multi-angle laser light scattering (MALLS) detector (Wyatt Technology, Santa Barbara, CA, USA), and an Optilab rEX refractive index detector (Wyatt Technology, Santa Barbara, CA, USA). The detection wavelength of HELEOS was set at 658 nm. Separations were performed using serially connected size exclusion columns (100 Å, 500 Å, 10³Å and 10⁴ Å Phenogel columns, 5 μm , 300 \times 7.8 mm, Phenomenex, Torrance, CA, USA) at 60 °C using DMF containing 0.1 M LiBr as the mobile phase. The MALLS detector was calibrated using pure toluene with no need for calibration using polymer standards and can be used for the determination of the absolute molecular weights (MWs). The MWs of polymers were determined based on the dn/dc value of each polymer sample calculated offline using the internal calibration system processed by the ASTRA V software (Version 5.1.7.3, Wyatt Technology, Santa Barbara, CA, USA). Circular dichroism (CD) measurements were carried out on a JASCO J-700 CD spectrometer. The polymer samples were typically prepared at

concentrations of 0.02-0.25 mg/mL for CD analysis unless otherwise specified. The solution was placed in a quartz cell with a path length of 0.2 cm and the mean residue molar ellipticity of each polymer was calculated based on the measured apparent ellipticity according to the reported formulas: Ellipticity ($[\theta]$ in $\text{deg cm}^2 \text{ dmol}^{-1}$) = (millidegrees \times mean residue weight)/(path length in millimeters \times concentration of polypeptide in mg ml^{-1}). The helicity of the polypeptides was calculated using the following equation: helicity = $(-[\theta_{222}] + 3,000)/39,000$.^[2] Lyophilization was performed on a FreeZone lyophilizer (Labconco, Kansas City, MO, USA).

Synthesis of Oleic Acid *N*-Hydroxysuccinimide Ester (Oleyl-NHS)

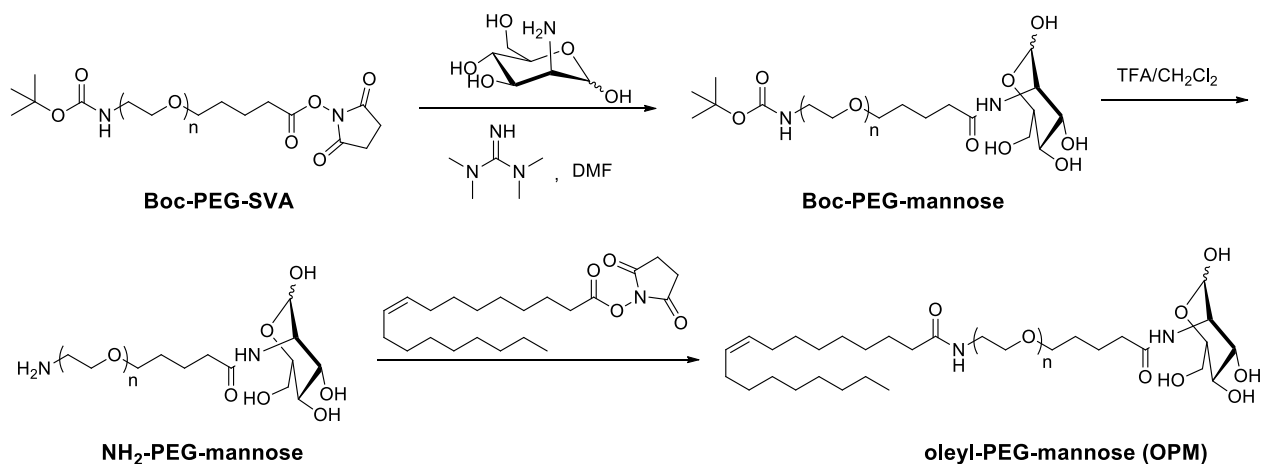
NHS (2.67 g, 23.2 mmol) and DIEA (2.72 mL, 15.6 mmol) were dissolved in THF (50 mL). The mixture was cooled in an ice bath to which oleoyl chloride (85%, 6.1 mL, 15.6 mmol) was added dropwise over the course of 1 h. The mixture was allowed to stir at 0 °C for 2 h and then overnight at room temperature. The grey precipitate was removed by centrifugation. After the solvent was removed under vacuum, the resulting yellowish oil was dissolved in DCM (20 mL) and washed with 5% HCl (10 mL \times 2). DCM was dried over MgSO_4 and then evaporated under vacuum to give the crude product. Oleyl-NHS was recrystallized from ethanol (yield 62%). $^1\text{H NMR}$ (CDCl_3 , 500 MHz): δ 5.34 (m, 2H, $\text{CH}=\text{CH}$), 2.84 (s, 4H, $\text{COCH}_2\text{CH}_2\text{CO}$), 2.60 (t, 2H, $\text{CH}_2\text{CH}_2\text{COON}$), 2.01 (m, 4H, $\text{CH}_2\text{CH}=\text{CHCH}_2$), 1.74 (m, 2H, $\text{CH}_2\text{CH}_2\text{COON}$), 1.44-1.24 (m, 20H, other CH_2), 0.87 (t, 3H, CH_3). ESI-MS (m/z): $\text{C}_{22}\text{H}_{37}\text{NO}_4\text{Na}$ ($\text{M}+\text{Na}$), calcd., 402.2; found, 402.2.

Synthesis and Characterization of Oleyl-Trimethyl Chitosan Chloride (OTMC)



Trimethyl chitosan chloride (TMC, MW = 200 kDa, quarternization degree of 28.7%) was synthesized as described previously.^[3] TMC (50 mg, 0.28 mmol of NH_2) and oleyl-NHS (10.6 mg, 0.028 mmol) were dissolved in dioxane/water (3 mL, 1:1, v/v), into which DMAP (34.1 mg, 0.28 mmol) and triethylamine (TEA) (80 μL , 0.56 mmol) were added. The solution was stirred overnight at room temperature. The resulting polymer was then precipitated by ethanol/ether/hexane (30 mL, 1:1:1, v/v/v). After being dissolved in water and precipitated by ethanol/ether/hexane (30 mL \times 3, 1:1:1, v/v/v), the product was dissolved in water and further purified by ultrafiltration (MWCO = 10 kDa). ^1H NMR was used to characterize the polymers (Supplementary Fig. S1). The quarternization degree was calculated by the integral ratio of trimethyl protons (c) to chitosan backbone C2-C6 protons (b). The oleyl conjugation degree was calculated by the integral ratio of oleyl protons (e) to trimethyl protons (c).

Synthesis and Characterization of Oleyl-PEG-Mannose (OPM)



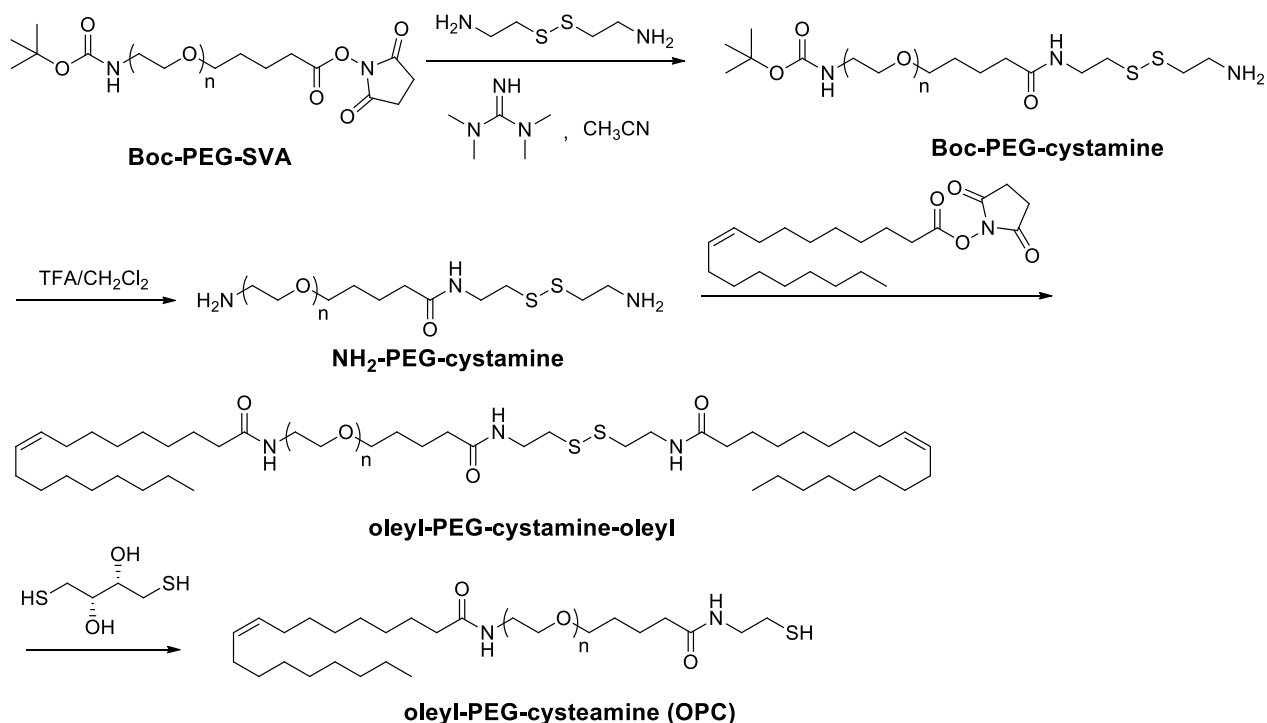
Boc-PEG-mannose was obtained by reacting Boc-PEG-SVA with D-mannosamine in DMF. D-mannosamine hydrochloride (108 mg, 0.50 mmol) and 1,1,3,3-tetramethylguanidine (120 μ L, 0.96 mmol) were dissolved in DMF (10 mL). The mixture was then added to a vial containing Boc-PEG-SVA (MW = 3.4 kDa, 340 mg, 0.10 mmol). The mixture was stirred for 48 h at 50 $^{\circ}$ C and dialyzed against DI water for 24 h (MWCO = 1 kDa). The product Boc-PEG-mannose was lyophilized (yield 74%) and characterized by MALDI-TOF-MS. Individual peak shifts (relative to Boc-PEG-SVA) corresponding to the deduction of one NHS group and the addition of one mannosamine per PEG were observed ($m/z = +64$).

Boc-PEG-mannose (250 mg, 0.07 mmol) was deprotected by TFA/DCM (5.0 mL, 1:1, v/v) to yield NH₂-PEG-mannose. The reaction was allowed to proceed for 1 h at room temperature. The polymer was then precipitated and washed with cold diethyl ether (20 mL \times 2, yield 86%). The product (NH₂-PEG-mannose) was characterized by MALDI-TOF-MS. Individual peak shifts (relative to Boc-PEG-mannose) corresponding to the deduction of one Boc group per PEG were observed ($m/z = -100$).

The final product OPM was synthesized by reacting oleyl-NHS (50.0 mg, 0.13 mmol), DIEA (30 μ L, 0.17 mmol) and NH₂-PEG-mannose (200 mg, 0.06 mmol) in 1,4-dioxane/DMF/H₂O (6.0 mL, 4:1:1, v/v/v). The solution was allowed to stir overnight at room

temperature, after which it was dialyzed against DI water for 24 h (MWCO = 1 kDa). OPM, the final product, was lyophilized (yield 68%) and characterized by MALDI-TOF-MS (Supplementary Figure S2). Individual peak shifts (relative to NH₂-PEG-mannose) corresponding to the addition of one oleyl group per PEG were observed ($m/z = +264$).

Synthesis and Characterization of Oleyl-PEG-Cysteamine (OPC)



Cystamine dihydrochloride (113 mg, 0.50 mmol) and 1,1,3,3-tetramethylguanidine (120 μL , 0.96 mmol) were dissolved in acetonitrile (10 mL). The solution was then added to a vial containing Boc-PEG-SVA (MW = 3.4 kDa, 340 mg, 0.10 mmol). The mixture was stirred overnight at room temperature and dialyzed against DI water for 24 h (MWCO = 1 kDa). The product, Boc-PEG-cysteamine, was lyophilized (yield 76%) and characterized by MALDI-TOF-MS. Individual peak shifts (relative to Boc-PEG-SVA) corresponding to the deduction of one NHS group and the addition of one cysteamine per PEG were observed ($m/z = +37$).

Boc-PEG-cystamine (250 mg, 0.07 mmol) was deprotected by TFA/DCM (5 mL, 1:1, v/v) to give NH₂-PEG-cystamine. The reaction was allowed to proceed for 1 h at room temperature. The polymer was then precipitated and washed with cold diethyl ether (20 mL × 2, yield 90%). The product was characterized by MALDI-TOF-MS. Individual peak shifts (relative to Boc-PEG-cystamine) corresponding to the deduction of one Boc group per PEG were observed ($m/z = -100$).

Oleyl-PEG-cystamine-oleyl was synthesized by reacting oleyl-NHS (50.0 mg, 0.13 mmol), DIEA (30 μL, 0.17 mmol) and NH₂-PEG-cystamine (200 mg, 0.06 mmol) in 1,4-dioxane/DMF/H₂O (6.0 mL, 4:1:1, v/v/v). The solution was stirred overnight at room temperature and dialyzed against DI water for 24 h (MWCO = 1 kDa). The product, Oleyl-PEG-cystamine-oleyl, was lyophilized (yield 72%) and characterized by MALDI-TOF-MS. Individual peak shifts (relative to NH₂-PEG-cystamine) corresponding to the addition of two oleyl groups per PEG were observed ($m/z = +529$).

The final product OPC was obtained by reacting oleyl-PEG-cystamine-oleyl (200 mg, 0.05 mmol) and DTT (11.0 mg, 0.07 mmol) in DI water (6.0 mL). The reaction was allowed to proceed overnight at room temperature and then dialyzed against DI water (MWCO = 1 kDa). The product was lyophilized (yield 82%) and characterized by MALDI-TOF-MS (Supplementary Figure S3). Individual peak shifts (relative to oleyl-PEG-cystamine-oleyl) corresponding to the deduction of one (2-oleamidoethyl)thio group per PEG were observed ($m/z = -340$).

Preparation and Characterization of SSNPs

siRNA and sodium tripolyphosphate (TPP) were dissolved in DEPC-treated water at 0.2 mg/mL and 1 mg/mL, respectively, and then mixed at the siRNA/TPP weight ratio of 1:12.5. OTMC, PVBLG-8, OPM, and OPC were separately dissolved in DEPC-treated water at 2 mg/mL, 1 mg/mL, 10 mg/mL, and 10 mg/mL, respectively and then mixed at the predetermined weight ratios of 5:1:5:5. Subsequently, the OTMC/PVBLG-8/OPM/OPC mixture was added to

siRNA/TPP at the OTMC/TPP weight ratio of 8:1 followed by vortexing for 30 s and incubation at 37 °C for 30 min. The obtained SSNPs were characterized for size and zeta potential using dynamic light scattering (DLS, Zetasizer Nano-ZS, Malvern). A gel retardation assay was used to evaluate siRNA condensation. Briefly, SSNPs or naked siRNA were loaded in 4% low-melting agarose gel followed by electrophoresis at 56 V for 1 h and visualization of siRNA migration by gel documentation. SSNPs were also characterized by SEM (4800, Hitachi, Japan). The stability of SSNPs against pH alteration, salt, and dilution was evaluated in terms of particle size and zeta potential. In order to evaluate the stability of SSNPs against salt and dilution, they were diluted with PBS (0.15 M, pH 6.8) up to 100-fold. To simulate the pH alteration in the gastrointestinal tract, the pH of the SSNPs suspension was adjusted to 1.2 using 1 N HCl and back to 6.8 using 1 N NaOH.

Stability of siRNA

In order to evaluate the *in vivo* stability of siRNA following oral administration, siRNA-containing SSNPs or naked siRNA was treated with mouse serum or intestinal fluids. Blood was collected from the orbital sinus of male C57BL/6 mice and centrifuged at 12,000 rpm for 4 min to separate the serum. To prepare the intestinal fluids, mice were sacrificed and the whole small intestine was washed with cold PBS (2 mL, 0.2 M, pH 7.4) through insertion of a sonde needle into the upper side and cannulation on the lower side. The washed solution was centrifuged at 12,000 rpm and 4 °C for 20 min, and the supernatant was collected as the intestinal fluids. SSNPs (0.2 mL) were mixed with mouse serum or intestinal fluids (0.2 mL). After incubation at 37 °C for 2 h, the mixture was heated at 80 °C for 5 min to deactivate the nucleases. Heparin (1000 U/mL) was added to dissociate the siRNA. The mixture was loaded on 4% agarose gel followed by electrophoresis at 56 V for 1 h and siRNA integrity visualization by gel documentation.

Mucoadhesion

SSNPs (400 μ L) were mixed with mucin solution (1 mL, 200 μ g/mL) and incubated at 37 °C for 8 h. The solution was centrifuged at 12,000 rpm for 10 min. The mucin adsorption level was determined by harvesting the supernatant and measuring the remaining mucin content with a colorimetric method using periodic acid/Schiff staining.^[4]

Permeation Studies in Human FAE and Non-FAE models

To establish the human non-FAE model, Caco-2 cells were seeded on Millicell[®] (pore size 0.4 μ m, surface area 0.6 cm², Millipore) at 5×10^4 cells/well and subsequently cultured for 21 days to form monolayers.⁵ The media at both the apical (AP) and basolateral (BL) sides were replaced daily. The transepithelial electric resistance (TEER) values of monolayers reached 300-350 Ω /cm² after the 21-day culture.

To establish the FAE model, Caco-2 cells were cultured on Millicell[®] for 16 days before Raji B cells were seeded on the BL side at 5×10^4 cells/well. The cells were co-cultured for another 7 days with media at the AP side being replaced daily. The TEER values of the co-cultured monolayers were similar to the mono-cultured cell monolayers (300-350 Ω /cm²), suggesting that the introduction of Raji cells did not alter the polarity of Caco-2 cells and the intercellular tight junctions^[5].

Cy3-siRNA containing SSNPs or naked Cy3-siRNA was added to the AP side of the FAE and non-FAE models in HBSS at 0.4 μ g Cy3-siRNA/well. At selected time intervals, transepithelial electrical resistance (TEER) was measured and an aliquot of 50 μ L was withdrawn from the BL side to quantify transported Cy3-siRNA. The apparent permeability coefficient (P_{app}) for Cy3-siRNA was calculated using the equation of $P_{app} = Q / Act$, where Q is the total amount of Cy3-siRNA permeated (ng), A is the diffusion area of the cell monolayers (cm²), c is the initial concentration of Cy3-siRNA on the AP side (ng/cm³), and t is the total time of the transport experiment (s).

After the 4-h transport study, Cy3-siRNA penetration/distribution in the cell monolayers was observed by CLSM (LSM 700, Zeiss, Germany) at optical sections with 5- μ m in increment.

The fluorescence intensity in each section was analyzed by Image J. To quantify the penetration of SSNPs, we defined the penetration depth as the distance from the periphery of the AP side to the site where the fluorescence intensity decreased by 95% as compared to the maximal fluorescent intensity of the SSNPs-treated cell monolayers at the apical periphery. The uptake level of Cy3-siRNA in the cell monolayers was also determined by lysing the monolayers with RIPA lysis buffer (500 μ L) and quantifying the Cy3-siRNA content in the lysate. Results were expressed as ng of Cy3-siRNA per mg of cellular protein.

The tight junction protein-associated transport mechanism was evaluated by immunostaining. After treatment of cell monolayers with SSNPs for 4 h, cells were fixed in 3.7% paraformaldehyde, washed with PBS for three times, and permeabilized with 0.2% Triton X-100 for 15 min at 37 °C. Cells were then washed with PBS and blocked with 1% bovine serum albumin (BSA) for 60 min at 37 °C. Subsequently, the cells were treated with mouse monoclonal anti-ZO-1-Alexa Fluor[®] 488 (Invitrogen, Grand Island, NY, USA) at 1:50 dilution for 60 min at 37 °C or with phalloidin-Alexa Fluor[®] 350 (Invitrogen, Grand Island, NY, USA) at 4 °C for 20 min. The stained cells were evenly mounted on slides and analyzed by using CLSM.

Cell Uptake

RAW 264.7 cells were seeded on 24-well plates at 5×10^4 cells/well and cultured for 24 h. The medium was replaced by serum-free DMEM (500 μ L), and Cy3-siRNA-containing SSNPs were added (0.4 μ g siRNA/well) before incubation at 37 °C for 4 h. Cells were washed with PBS three times and then lysed with the RIPA lysis buffer (500 μ L). The quantity of Cy3-siRNA in the lysate was determined by spectrofluorimetry ($\lambda_{ex}=480$ nm, $\lambda_{em}=520$ nm); the total protein content was determined by BCA assay. Uptake level was expressed as the amount of Cy3-siRNA per mg of cellular protein. In order to elucidate the effect of mannose-receptor recognition during nanoparticle internalization, cell uptake study was performed in serum-free DMEM supplemented with 100, 300, and 600 μ mol/L of mannose, respectively. Internalization and intracellular distribution of Cy3-siRNA in RAW 264.7 cells was also visualized by CLSM (700,

Zeiss, Germany) following nanoparticle treatment, fixation with 4% paraformaldehyde (PFA), and nuclei-staining with DAPI.

To explore the mechanisms involved in the uptake process, cells were pre-incubated with endocytic inhibitors including NaN₃ (200 mM)/deoxyglucose (50 mM), chlorpromazine (10 µg/mL), genistein (200 µg/mL), methyl-β-cyclodextrin (mβCD, 50 µM), and wortmannin (50 nM) for 30 min prior to nanoparticle application and throughout the 4 h uptake experiment at 37 °C. Results were expressed as percentage uptake of the control where cells were incubated with SSNPs at 37 °C for 4 h. To further explore the caveolae-mediated endocytosis, RAW 264.7 cells were incubated with Cy3-siRNA-containing SSNPs and FITC-CTB (5 µg/mL) for 2 h before CLSM observation. To evaluate the clathrin-mediated pathway, RAW 264.7 cells were incubated with Cy3-siRNA-containing SSNPs and transferrin-Alexa Fluoro 635 (10 µg/mL) for 2 h before the analysis by CLSM.

***In Vitro* TNF-α Knockdown in Macrophages**

RAW 264.7 cells were seeded on 24-well plates at 5×10^4 cells/well and cultured for 24 h. The medium was changed to serum-free DMEM and siRNA-containing SSNPs were added at pre-determined siRNA concentrations. Following incubation for 4 h, the medium was replaced with serum-containing DMEM and cells were further cultured for 20 h before LPS stimulation ($100 \text{ ng} \cdot \text{mL}^{-1}$) for 3 h. Extracellular TNF-α production was quantified by ELISA (R&D Systems, MN, USA). The TNF-α mRNA level was monitored by real-time PCR. The silencing efficiency was denoted as the percentage of TNF-α or TNF-α mRNA levels of the control cells which did not receive nanoparticle treatment. To prepare samples for real-time PCR analysis, RNA was isolated from cells using Trizol reagent (Invitrogen). cDNA was synthesized from 500-ng total RNA using the high capacity cDNA reverse transcription kit (Applied Biosystems, Carlsbad, CA, USA) according to the manufacturer's suggested protocol. Synthesized cDNA, TNF-α primers (forward and reverse, Supplementary Table S2), and SYBR Premix Ex Taq™ were mixed and run on the ABI PRISM 7900HT Real-Time PCR system (Applied Biosystems, Carlsbad, CA,

USA). Sequences of the primers used were designed with Primer Bank (Supplementary Table S2). The ribosomal mRNA actin was used as an internal loading control, and its expression did not change over the 24 h period following addition of LPS, SSNPs, or siRNA.

Supplementary Table S2. Forward (F) and Reverse (R) TNF- α primer sequences.

Primer	Sequence
TNF- α F	CCACCACGCTCTTTCTGTCTACTG
TNF- α R	GGGCTACAGGCTTGTCACCTCG

Cytotoxicity of SSNPs

Caco-2 and RAW 264.7 cells were seeded on 96-well plates at 1×10^4 cells/well and cultured for 24 h before media replacement with serum-free DMEM (100 μ L/well). SSNPs were added at final siRNA concentrations of 0.05, 0.1, 0.2, 0.5, and 1 μ g/well. Following incubation for 4 h, the medium was removed and serum-containing DMEM was added. Cells were further cultured for 20 h before viability assessment by the MTT assay.

Oral Delivery of SSNPs Induced *in vivo* RNAi against Systemic Inflammation

TNF- α siRNA-containing SSNPs were orally gavaged to mice at 200 μ g siRNA/kg (4 mice per group) with untreated mice serving as a control group. The gavage volume was 0.39 mL/mouse at the animal body weight of 20 g. Twenty-four hours post administration, LPS (12.5 μ g/kg) and D-GalN (1.25 g/kg) were i.p. injected. Blood was collected 1.5 h later to determine the serum TNF- α level by ELISA. For direct comparison with i.v. injection, SSNPs were also i.v. injected to mice at various siRNA doses.

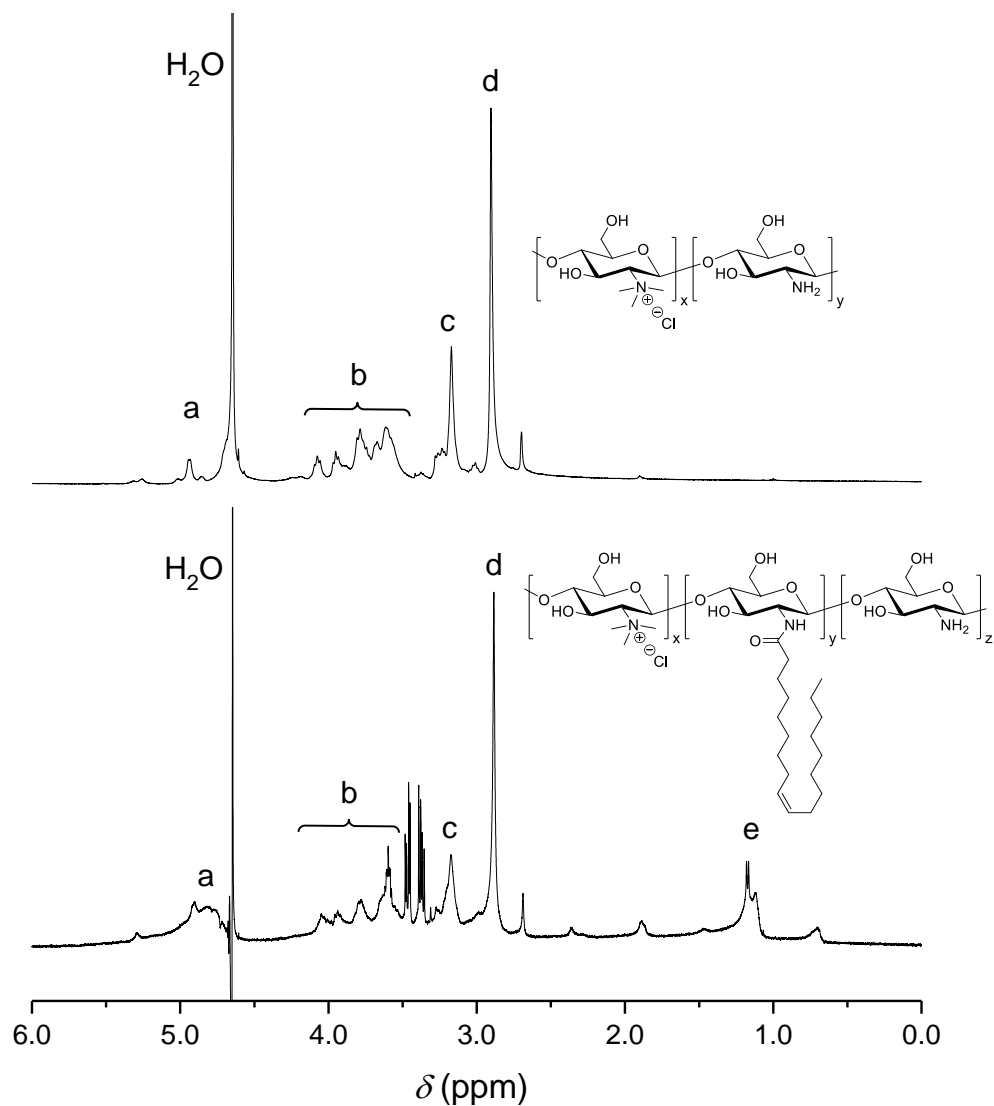
In another experiment, mice were orally gavaged with SSNPs and i.p. challenged with LPS/D-GalN as described above. Five hours post LPS/D-GalN stimulation, blood was collected to evaluate the serum ALT as well as AST levels using commercial kits (Biovision Inc., San

Francisco, CA, USA). Mice were then sacrificed. Liver, spleen, and lung were harvested, cut into small pieces, washed with saline, and homogenized with Trizol reagent. RNA extraction was performed as described for RAW 264.7 cells. Intracellular TNF- α mRNA levels were monitored by real-time PCR. For histological evaluation, mouse liver was also harvested 5 h post LPS/D-GalN stimulation, fixated in paraffin, cross-sectioned, and stained with haematoxylin/eosin (HE).

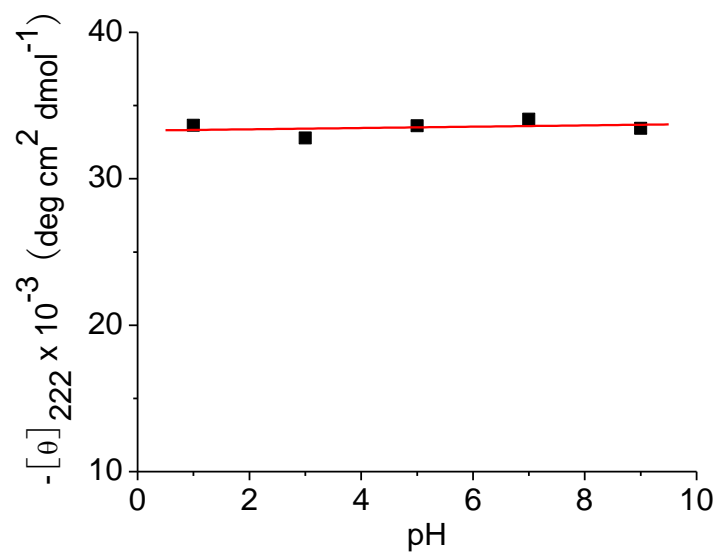
To evaluate the oral absorption and biodistribution profiles, SSNPs containing DY800-siRNA were orally gavaged to mice at 200 μ g siRNA/kg (3 mice per group). Mice were sacrificed 2 h post administration, and the liver, spleen, lung, and small intestine were harvested, washed with PBS, and fixed in 10% formalin before quantification of the fluorescent intensity in each organ using an Odyssey infrared mouse imaging system (800 nm emission). Organs from non-treated mice served as the blank. Biodistribution level in each organ was calculated from the calibration curve and represented as ng siRNA per gram tissue.

For lethality tests, mice (10 per group) were orally gavaged with SSNPs (200 μ g siRNA/kg) or PBS. Twenty-four hours later, LPS/D-GalN was i.p. injected as described above. The survival of animals was monitored for 24 h. Mice that received orally administered SSNPs without i.p. injection of LPS/D-GalN served as the control.

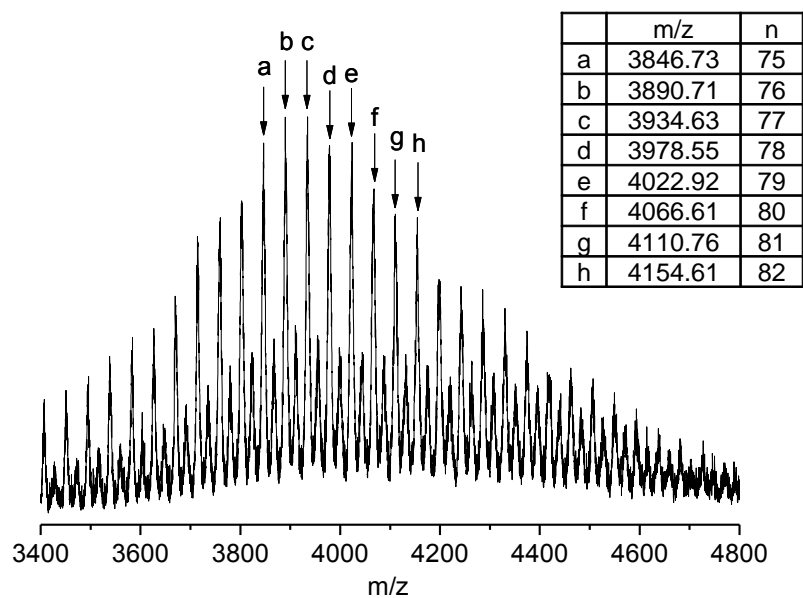
Supplementary Figures



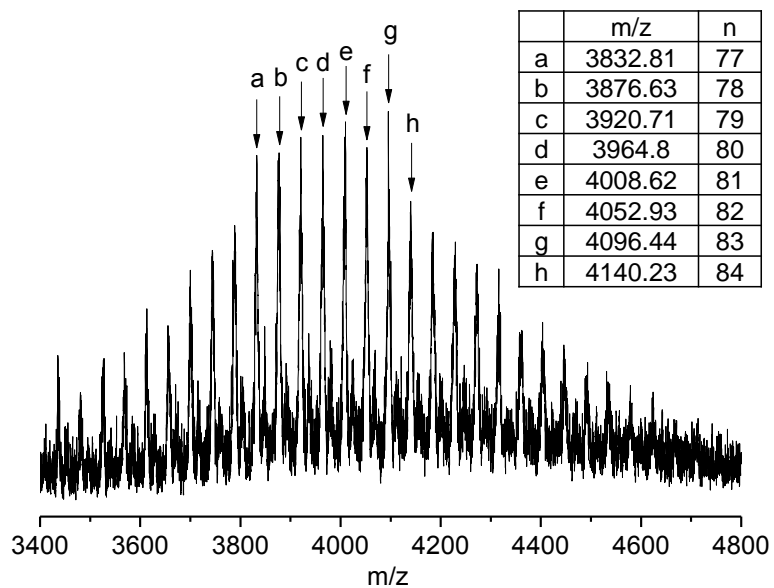
Supplementary Figure S1. ¹H NMR spectra of TMC and OTMC. (a) chitosan backbone C1 proton; (b) chitosan backbone C2-C6 protons; (c) trimethyl protons; (d) dimethyl protons; (e) oleyl protons. OTMC spectrum was obtained with water suppression. The quarternization degree was calculated by the integral ratio of (c) to (b); the oleyl conjugation degree was calculated by the integral ratio of (e) to (c).



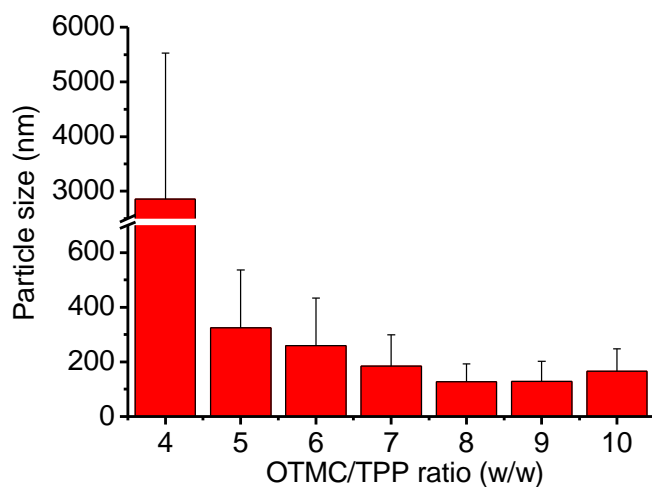
Supplementary Figure S2. pH-dependent helicity of PVBLG-8.



Supplementary Figure S3. MALDI-TOF MS analysis of oleyl-PEG_n-mannose (OPM). The obtained m/z is identical to the calculated m/z of OPM ($542.75 + 44.05 \times n$).

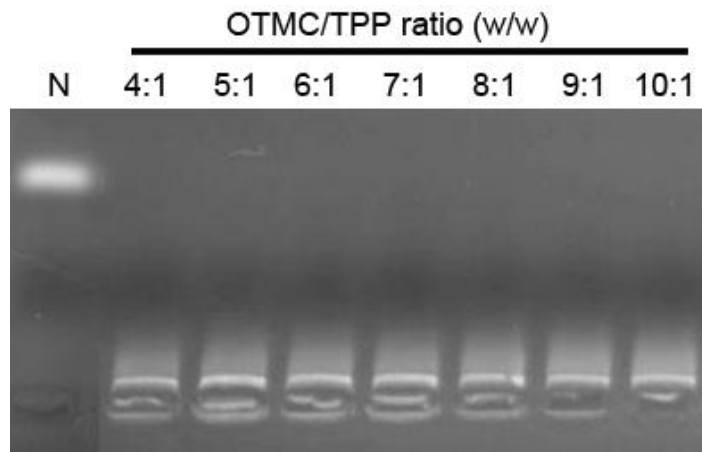


Supplementary Figure S4. MALDI-TOF MS analysis of oleyl-PEG_n-cysteamine (OPC). The obtained m/z is identical to the calculated m/z of OPM ($440.73 + 44.05 \times n$).

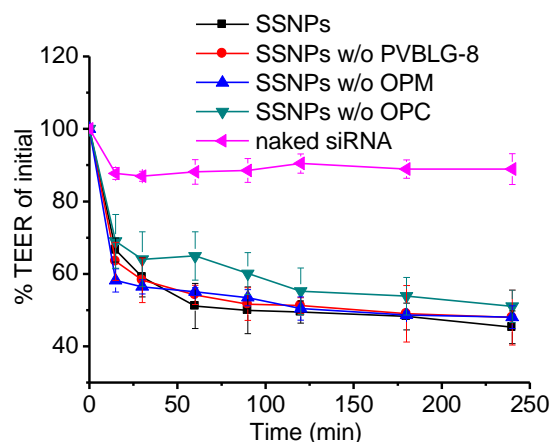


Supplementary Figure S5. Size and Zeta potential of SSNPs as a function of OTMC/TPP weight ratios.

The short length as well as linearity of siRNA often causes weak interaction with polycations, thus necessitating the use of large excessive amount of polycations to encapsulate siRNA. For the SSNPs, excessive polycations (OTMC and PVBLG-8) were used for effective siRNA encapsulation. The excessive amount of polycations may counteract the competitive siRNA replacement induced by anionic components in the physiological fluids. Additionally, excessive polycations (especially PVBLG-8 with membrane activity) could strengthen the interaction with oppositely charged cell membranes to enhance the siRNA internalization level.

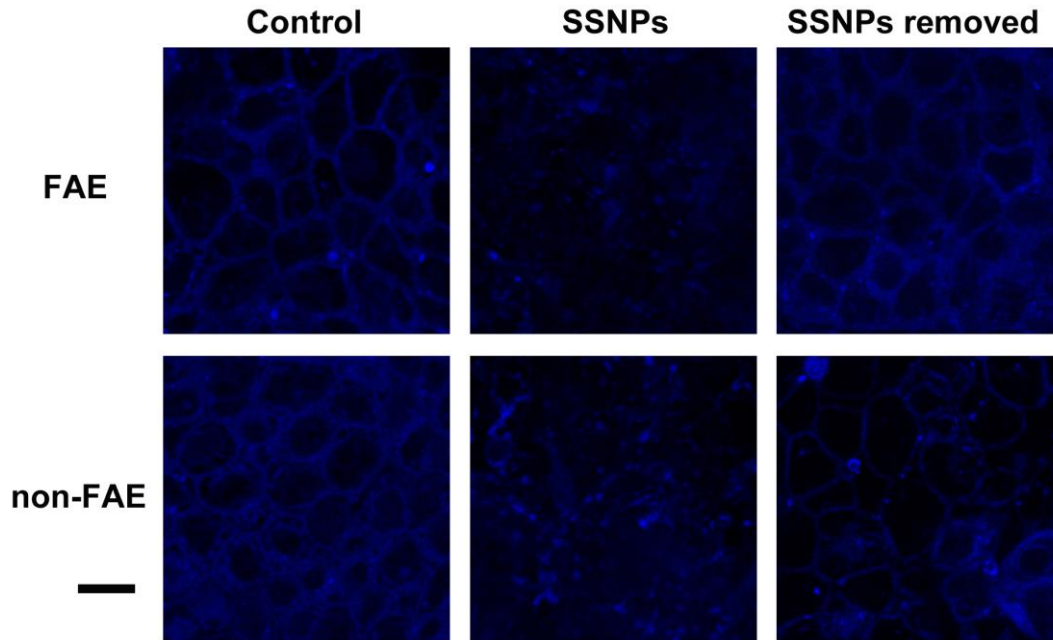


Supplementary Figure S6. Gel retardation assay showing siRNA migration in 4% agarose gel (N = naked siRNA). SSNPs were prepared at various OTMC/TPP weight ratios.

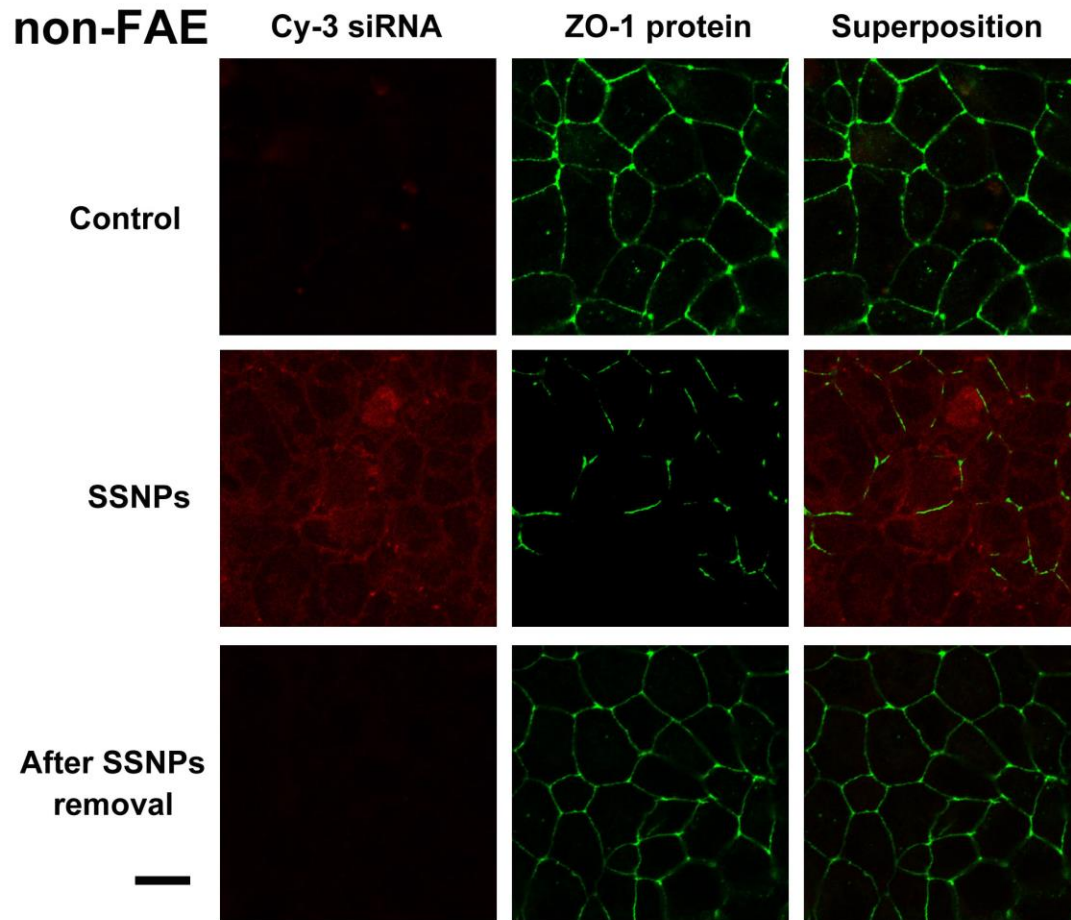


Supplementary Figure S7. TEER values of the human non-FAE model following incubation with SSNPs.

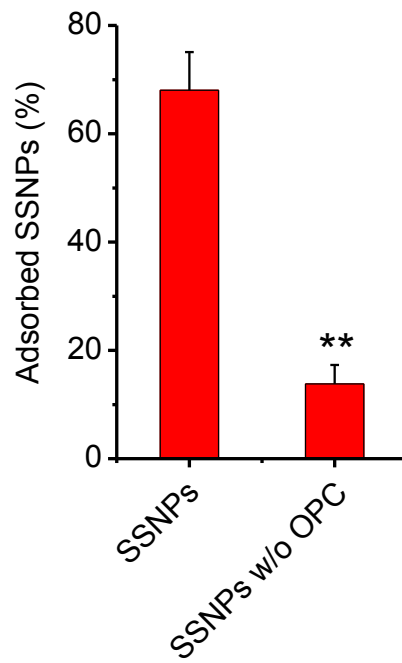
The ability of SSNPs to open TJs was not significantly altered by excluding OPM, OPC or PVBLG-8 from the SSNPs (Fig. 2D and Supplementary Fig. S7). Since removal of the components did result in reduced siRNA transport (Fig. 2D), it was suggested that the paracellular pathway made relatively low contributions to the translocation of SSNPs. For such evaluation, the Caco2-HT29MTX model ^[6] would be more suitable, because enterocytes are interspersed by goblet cells and mucus is secreted by HT29MTX cells on the apical surface, which more closely mimics the *in vivo* environment. The mucus layer will increase the distance between SSNPs and the cell monolayers, which may prevent the SSNPs from interacting with tight junctions and thus decrease the tight junction opening capacity.^[7] However, the tight junctions are partially interrupted by goblet cells, which will in turn promote the paracellular transport. The mucoadhesive property of SSNPs allows disulfide bonding with the mucus layer as well as cellular membranes, which can facilitate the accumulation of SSNPs in the mucus layer or on cell surfaces to subsequently improve the transcellular uptake in a concentration-driven manner.^[8] No mucus layers are lining up the M cells, and therefore may not influence the M cell uptake.



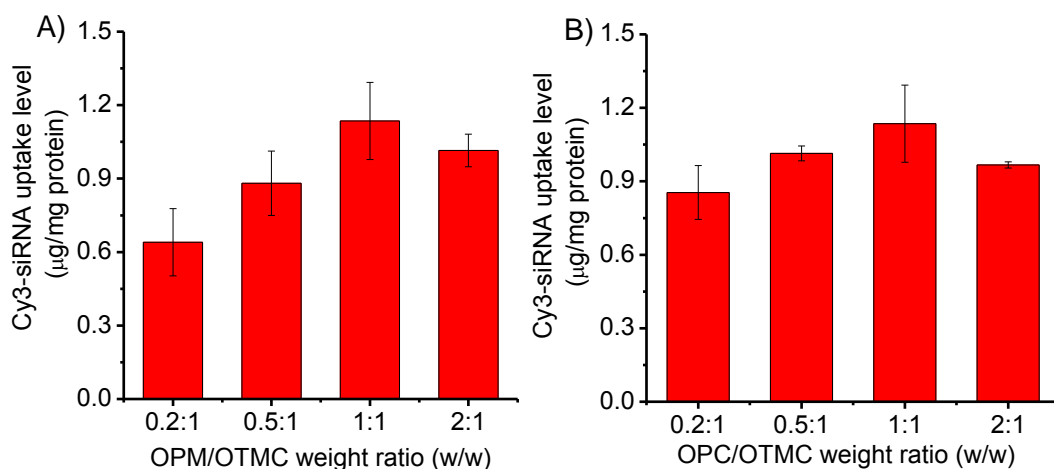
Supplementary Figure S8. F-actin distribution in FAE and non-FAE models following treatment with SSNPs for 4 h and further incubation for 24 h after SSNPs are removed. (bar = 20 μm).



Supplementary Figure S9. ZO-1 in the non-FAE model following treatment with SSNPs for 4 h and further incubation for 24 h after SSNPs are removed. (bar = 20 μ m).

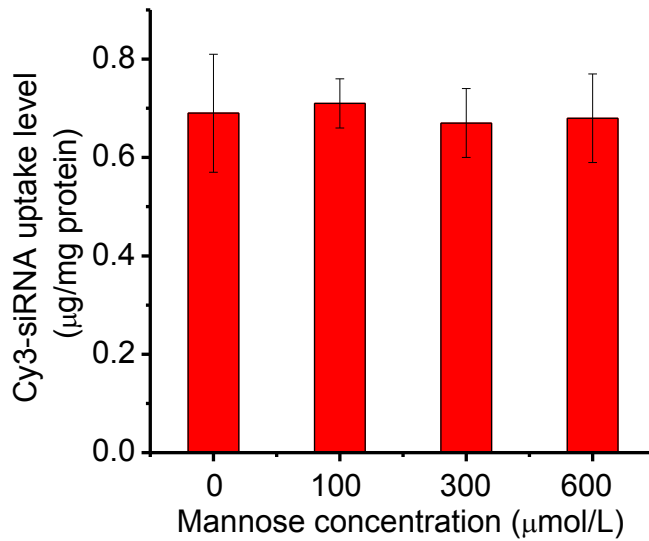


Supplementary Figure S10. Mucoadhesion of SSNPs as determined by the mucin adsorption assay. ** $p < 0.01$ v.s. SSNPs.



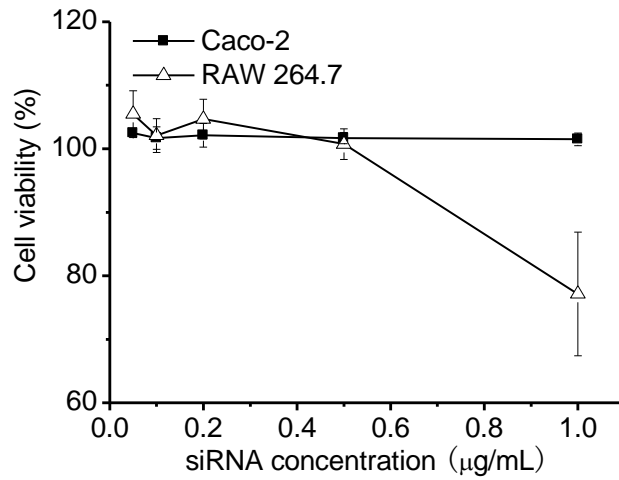
Supplementary Figure S11. Effect of OPM (A) and OPC (B) content on the cell uptake level of Cy3-siRNA-containing SSNPs in RAW 264.7 cells following 4-h treatment. OPC content was kept constant at the OPC/OTMC weight ratio of 1:1 when OPM content was increased from 0.2:1 to 2:1 (A), and vice versa (B).

The cell uptake level was enhanced as the relative OPM or OPC content in SSNPs was increased up to OPM/OTMC or OPC/OTMC weight ratio of 1:1, indicating that OPM and OPC were incorporated into the SSNPs to allow mannose receptor-mediated targeting and disulfide-mediated cell binding. However, when the OPM/OTMC or OPC/OTMC amount was further increased, the uptake level was not increased while slightly decreased, which could be attributed to the competitive targeting/binding with SSNPs as induced by free OPM or OPC.



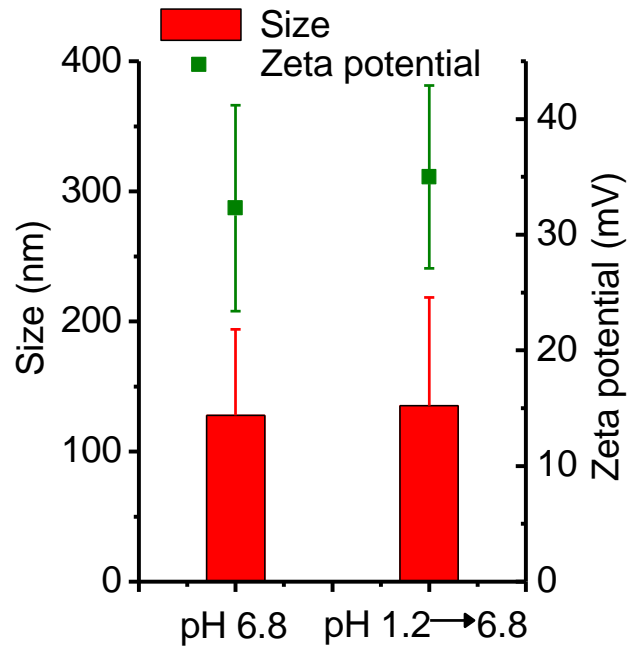
Supplementary Figure S12. Uptake of Cy3-siRNA-containing SSNPs w/o OPM in RAW 264.7 cells following incubation for 4 h in the presence of mannose (n = 3).

Free mannose showed unappreciable inhibitory effect on the uptake of non-targeted SSNPs without OPM (Supplementary Fig. S12), which further substantiated that the targeting effect of SSNPs towards macrophages was mediated by mannose-receptor recognition.

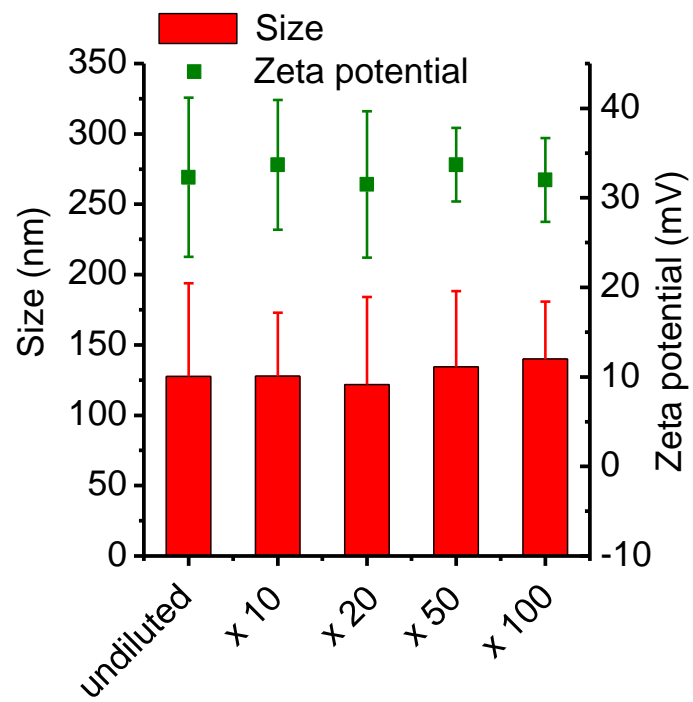


Supplementary Figure S13. Cytotoxicity of SSNPs in RAW 264.7 and Caco-2 cells (n = 3).

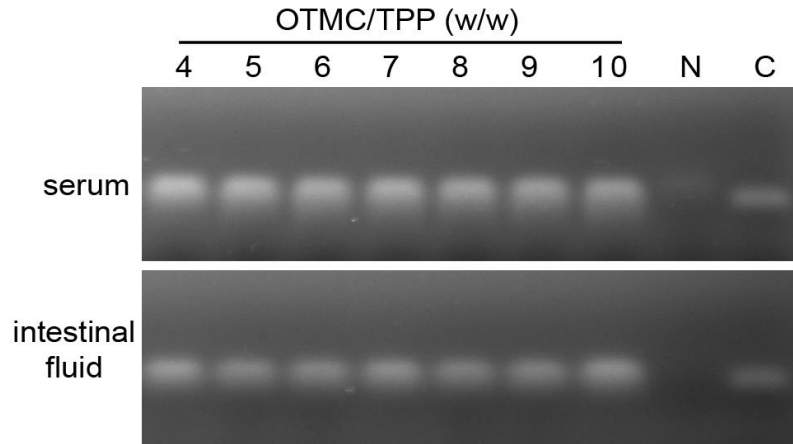
Minimal cytotoxicity was noted for SSNPs at the siRNA concentration no higher than 0.5 µg/mL (Supplementary Fig. S13), suggesting the desired cell tolerability of SSNPs.



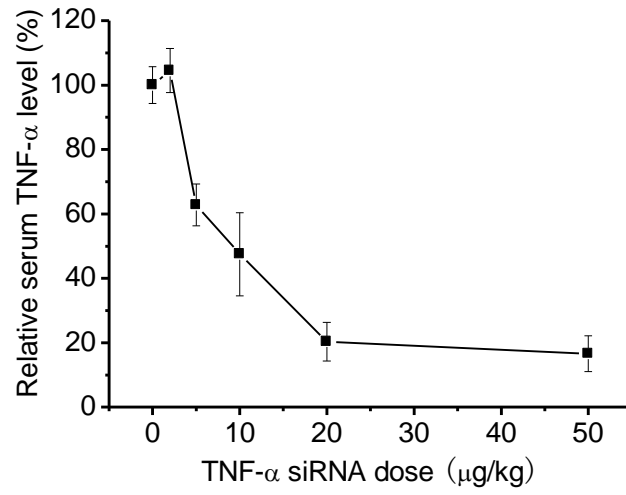
Supplementary Figure S14. Stability of SSNPs towards pH alteration from 6.8 to 1.2 and back to 6.8.



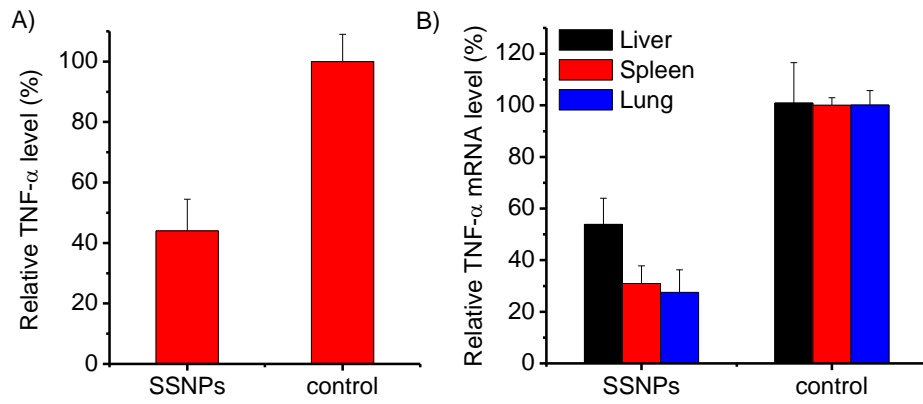
Supplementary Figure S15. Stability of SSNPs following dilution with PBS for different folds.



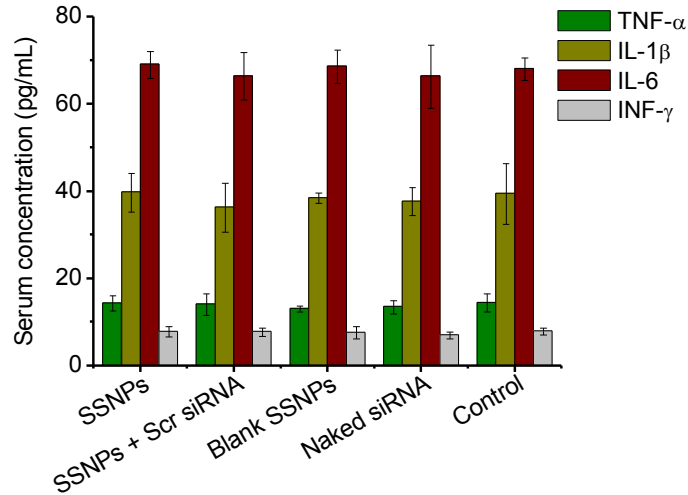
Supplementary Figure S16. siRNA stability in mouse serum and intestinal fluids at various OTMC/TPP ratios.



Supplementary Figure S17. TNF- α silencing efficiency of SSNPs following i.v. injection (n = 3).



Supplementary Figure S18. Serum TNF- α level (A) and TNF- α mRNA levels in the liver, spleen, and lung (B) following oral administration of SSNPs at 50 μ g siRNA/kg (n = 3).



Supplementary Figure S19. Serum TNF- α , IL-1 β , IL-6, and INF- γ levels of mice 24 h after oral administration of SSNPs (200 μ g siRNA/kg) as determined by ELISA (n = 4). Control represents untreated normal mice.

It was shown that 24 h after oral administration of TNF- α siRNA containing SSNPs, Scr siRNA-containing SSNPs, blank SSNPs, and naked TNF- α siRNA, the serum (interleukin-1 β) IL-1 β , (interleukin-6) IL-6, TNF- α , and (interferon- γ) IFN- γ levels were not significantly increased compared to control mice receiving no treatment ($p > 0.05$, Supplementary Fig. S19). These results preliminary indicated that oral administration of SSNPs would not activate pro-inflammatory cytokines or induce IFN- γ responses.

References:

- [1] N. P. Gabrielson, H. Lu, L. C. Yin, D. Li, F. Wang, J. J. Cheng, *Angew Chem Int Edit* **2012**, *51*, 1143.
- [2] J. A. Morrow, M. L. Segall, S. Lund-Katz, M. C. Phillips, M. Knapp, B. Rupp, K. H. Weisgraber, *Biochemistry* **2000**, *39*, 11657.
- [3] L. C. Yin, J. Y. Ding, C. B. He, L. M. Cui, C. Tang, C. H. Yin, *Biomaterials* **2009**, *30*, 5691.
- [4] P. He, S. S. Davis, L. Illum, *Int J Pharmaceut* **1998**, *166*, 75.
- [5] S. Kerneis, A. Bogdanova, J. P. Kraehenbuhl, E. Pringault, *Science* **1997**, *277*, 949.
- [6] Y. H. Loo, C. L. Grigsby, Y. J. Yamanaka, M. K. Chellappan, X. Jiang, H. Q. Mao, K. W. Leong, *J Control Release* **2012**, *160*, 48.
- [7] K. M. Wood, G. M. Stone, N. A. Peppas, *Acta Biomater* **2010**, *6*, 48.
- [8] S. Cohen, G. Coue, D. Beno, R. Korenstein, J. F. J. Engbersen, *Biomaterials* **2012**, *33*, 614.